First measurement of the gravitational quadrupole moment of a blackwidow companion in PSR J2051-0827

Guillaume Voisin, C J Clark, R P Breton, V. Dhillon, M R Kennedy, D Mata-Sánchez

MNRAS **000**, 1–5 (2015) Preprint 3 January 2020 Compiled using MNRAS LATEX style file v3.0

First measurement of the gravitational quadrupole moment of a blackwidow companion in PSR J2051-0827

Guillaume Voisin[1,2]★, C. J. Clark,[1], R. P. Breton[1], V. S. Dhillon [3], M. R. Kennedy[1], D. Mata-Sánchez[1],

[1] *Jodrell Bank Centre for Astrophysics, School of Physics and Astronomy, The University of Manchester, Manchester M19 9PL, UK*
[2] *LUTH, Observatoire de Paris, PSL Research University, 5 Place Jules Janssen, 92195 Meudon, France*
[3] *Department of Physics and Astronomy, University of Sheffield, Sheffield S3 7RH, UK*

Accepted XXX. Received YYY; in original form ZZZ

ABSTRACT

We present the first measurement of the gravitational quadrupole moment of the companion star of a spider pulsar, namely black widows and redbacks, using pulsar timing data for blackwidow PSR J2051-0827. To this end we have used a new timing model which is able to account for periastron precession caused by tidal and centrifugal deformations of the star as well as by general relativity. Simultaneously, the model allows for a time-varying component of the quadrupole moment, thus self-consistently accounting for the ill-understood orbital period variations observed in these systems. Our analysis results in the first unambiguous detection of orbital eccentricity in this system with $e = 4.2 \pm 0.1 \cdot 10^{-5}$, together with a total precession of $-68.6^{+0.9}_{-0.5}$ deg/yr. We show that the variable quadrupole component is about 100 times smaller than the sum of the tidal and centrifugal components. We demonstrate how precise optical light curves of the companion star will allow to derive its apsidal motion constant from our results.

Key words: keyword1 – keyword2 – keyword3

1 INTRODUCTION

Spider pulsars are binaries composed of a millisecond pulsar primary and a low-mass non-degenerate secondary orbiting with a sub-day period that is often as short as a few hours. In the event that the companion has a very low mass, $< 0.1\,M_\odot$, the system is called a black widow. Those with heavier companions (0.1–$0.4\,M_\odot$) are called redbacks. These binaries are named after two spider species which share the characteristic that the larger female (occasionally) eats the smaller male after mating. Their astrophysical counterparts rather seem to proceed in a slow evaporation of the companion star by the pulsar after the latter mate has been recycled by the former, i.e. spun up to millisecond period through mass transfer Alpar et al. (1982). The fate of the companion, although as yet uncertain, would appear all the more cruel that there is evidence for the rejuvenation of some spider pulsars to have been particularly efficient with the two fastest known spinning pulsars being respectively a redback, PSR 1748-2446ad (Hessels et al. 2006), and a blackwidow, PSR J0952-0607 (Bassa et al. 2017). The observed similarity of the companion with low-mass X-ray binary secondaries as well as the transition of some redback systems (Archibald et al. 2009; Papitto et al. 2013; Bassa et al. 2014) to and from accreting states certainly supports the idea of these systems being the missing links in millisecond pulsar evolution, unless they form a separate and exotic category on their own (Chen et al. (2013); Benvenuto et al. (2012)). Probing the internal state of the companion, through a measurement of its gravitational quadrupole moment, thus represents an invaluable constraint for stellar evolution models.

The high potential of spider pulsars Roberts (2012) for timing is often hindered by their ill-understood orbital period variations, which are usually attributed to fluctuations of their quadrupole momentum caused by stellar magnetic cycles as proposed in (Applegate 1992) and later refined in e.g. Lanza & Rodonò (1999); Lanza (2006); Völschow et al. (2018); Navarrete et al. (2019). If quadrupole changes are responsible for the observed orbital period variations, then it is possible to design a dynamical model of the binary that includes this contribution. Nonetheless, such variations are only perturbations of a larger quadrupole moment due to the well-known centrifugal and tidal forces. However, the main effect that these latter components generate is an orbital precession which is only detectable if a significant eccentricity is present. This characteristic is made unlikely by the assumed evolution scenario where strong circularising mech-

★ E-mail: guillaume.voisin@manchester.ac.uk; astro.guillaume.voisin@gmail.com

anisms are expected (see Voisin et al. (2019) and references therein).

We recently showed (Voisin et al. 2019) that a perturbed orbit cannot be perfectly circular as a direct consequence of the well-known Bertrand's theorem which stipulates that only the harmonic and Newtonian potentials can lead to periodic motion. We demonstrated that in the case of spider systems, this property is effectively embodied in an apparent eccentricity and periastron precession. Owing to the estimated magnitude of quadrupole deformation, it was shown that the minimal value of that effective eccentricity may fall well within a detectable range.

In this letter, we report on the application of our model to blackwidow PSR J2051-0827. We reanalysed the timing data published in Shaifullah et al. (2016) using an implementation of the model of Voisin et al. (2019).

2 THE TIMING MODEL

The timing model presented in Voisin et al. (2019) is an extension of the relativistic binary model of Damour & Deruelle (1985, 1986) to binaries with a companion deformed by tidal and centrifugal forces in the limit of quasi-circular orbits i.e. the model is accurate to first order in eccentricity. The model comes with the restriction that the spin of the companion is assumed to be synchronized with its orbital motion such that the axis of the deformation remains constant. In addition, a time-varying component is allowed to account for orbital period variations. Thus, binary dynamics derives from the companion gravitational potential $\Phi_c = -\frac{Gm_c}{r}\left(1 + (J_s + J_v(t) + J_t\frac{a^3}{r^3})\frac{a^2}{r^2}\right)$ where m_c is the mass of the companion, J_s, J_t and $J_v(t)$ are dimensionless parameters quantifying the spin, tidal and variable quadrupole components respectively, G is the gravitational constant, a the separation between the pulsar and its companion at a reference time and r the distance between the two objects (Voisin et al. 2019). The quadrupole parameters are related to the quadrupole moment along the radial axis Q_{rr} by $\frac{3}{2}\frac{Q_{rr}}{m_c a^2} = J_s + J_v(t) + J_t\frac{a^3}{r^3}$. Relativistic corrections at the first post-Newtonian order are included as in, e.g., Damour & Deruelle (1985), and contribute terms of order $\epsilon = \frac{GM}{ac^2}$ where $M = m_c + m_p$ is the total mass of the system, m_p the mass of the pulsar, and a is the binary separation.

One can show that the tidal and quadrupole numbers are connected by the relation $J_s = (1+q)J_t/3$, where $q = m_c/m_p$ is the mass ratio of the system. Using equilibrium tide theory (Sterne 1939; Kopal 1978), one can relate these numbers to the apsidal motion constant k_2,

$$J_t = -k_2\rho_f^5 f^5 q^{-1}, \tag{1}$$

where $\rho_f = R_f/a$, R_f is the volume-averaged Roche-lobe radius, and f the filling factor of the companion such that $R_c/a = f\rho_f$. It is convenient to use the formula $\rho_f = 0.49q^{2/3}/\left(0.6q^{2/3} + \ln\left(1+q^{1/3}\right)\right)$ (Eggleton 1983). The apsidal motion constant depends on integration of the stellar structure, and in particular on the equation of state of the star. The variable component is left as a free parameter which is related to the orbital frequency derivatives $f_b^{(i)} = \mathrm{d}^i f_b/\mathrm{d}t^i(T_a)$ like so,

$$J_v(t) = -\frac{1}{6f_b}\sum_{i=0}\frac{f_b^{(i)}}{i!}(t-T_a)^i, \tag{2}$$

where $f_b = 1/P_b$ is the orbital frequency at the time of ascending node T_a. Interestingly, this translates into $J_v(t) = -\frac{1}{6}\frac{\Delta P_b}{P_b}$ where ΔP_b is the orbital period variation.

Together with relativistic effects, quadrupole deformations are responsible for a minimum eccentricity,

$$e_{\min} = -J_t(16+q) + \frac{\epsilon}{2}\left(\frac{m_c m_p}{M} + 3\right). \tag{3}$$

The total eccentricity that may be detected in timing observations is the sum of this minimum component and the traditional, hereafter Keplerian, component : $e = e_{\min} + e_K$. The Keplerian component is the one that may be nullified by circularisation processes. On the other hand, $e_{\min}$ should be considered as an effective, as opposed to geometrical, component. In any case, if the eccentricity e is large enough to be detected then one also has to account for orbital precession at an angular rate of

$$\dot{\omega} = n_b\,(15J_t + 3J_s + 3\epsilon) \tag{4}$$

where $n_b = 2\pi f_b$. The first term of equation (4) gives the tidal contribution $\dot{\omega}_{\rm tid}$, the second the spin contribution $\dot{\omega}_{\rm spin}$ and the third term is the relativistic contribution $\dot{\omega}_{\rm rel}$.

Since spiders are close binaries, the model only includes the so-called Rœmer delay, namely the geometrical delay induced by the variation of the distance projected along the line of sight of the observer as the pulsar circles its orbit. Relativistic delays such as the effects of time dilation or light bending may safely be neglected (Voisin et al. 2019). It follows that the inclination angle of the orbital plane cannot be measured independently from the pulsar semi-major axis, but only the projection of the latter along the line of sight $x = a_p \sin i$. Additionally, information on the masses of the two stars is limited to the so-called mass function $(m_c \sin i)^3/(m_p + m_c)^2 = G^{-1}x^3 n_b^2$.

Although one may neglect the relativistic contributions in first approximation, one sees that the mass ratio q remains absolutely necessary to derive the apsidal motion constant k_2 from equations (4) and (1). If relativistic corrections are to be included, then the knowledge of both masses is necessary (or of one mass and the inclination and using the mass function). Furthermore, the knowledge of the filling factor f is certainly the most sensitive parameter needed to derive the apsidal motion constant, as it comes in equation (1) to the fifth power. This factor cannot in general be obtained through the technique of pulsar timing, but can instead be extracted from modelling of the optical light curve of the companion (e.g. Breton et al. 2013). The same technique can inform us on the orbital inclination, and thus partially lift the degeneracy of the mass function. The mass ratio can be obtained through optical spectroscopy (e.g. van Kerkwijk et al. 2011) by measuring the velocity of the companion along the line of sight and comparing it to the projected pulsar velocity derived from timing. If spectroscopic observations are not available, light-curve modelling can provide constraints on the masses of the system but usually with very large uncertainties. As a last resort, one can estimate the range of allowed mass ratios by assuming peculiar pulsar masses typically in the range $1.4M_\odot \leq m_p \leq 2.5M_\odot$.

3 RESULTS AND DISCUSSION

We here re-analyse 21 years of timing data previously published in Shaifullah et al. (2016)[1] using a version of the ELL1 timing model of the Tempo2 pulsar timing software (Hobbs et al. 2006; Edwards et al. 2006) modified according to the prescriptions of Voisin et al. (2019)[2]. The uncertainties were estimated using the affine-invariant Markov-Chain-Monte-Carlo (MCMC) algorithm of Goodman & Weare (2010); Foreman-Mackey et al. (2013)[3].

The mean values of the parameter posterior distribution functions are given in table 1. Compared to the fit using Tempo2's BTX model presented in Shaifullah et al. (2016), the reduced χ^2 is significantly improved (4.06 against 4.2) although our fit uses 3 extra parameters (κ_c, κ_s and $\dot{\omega}$). Some of the parameters common to both fits are significantly different, the largest discrepancy occurring in the spin frequency which is different by ~ 57 standard deviations, which indicates that when precession and eccentricity are not accounted for the spin frequency f adjusts to partly compensate. The orbital parameters $x, \dot{x}, T_{\rm asc}, f_b$ are consistent within 2σ. The orbital period derivatives show similar but nonetheless significantly different values between the two fits (see below). This might be due to the large correlations between each of these parameters (see corner plot in online material). The 1σ error bars themselves are quite different between the BTX fit and the present one, which is partly the result of the different methods used: Tempo2 returns an estimate based on its least-square fit while we use here a MCMC sampling of the posterior distribution function. Moreover, we note that the large reduced χ^2 we obtain is either due to un-modelled effects or to underestimated uncertainties on the times of arrival. In the latter case, the error bars given in table 1 should be multiplied by ~ 2, particularly since the marginalised posterior distributions of all parameters are closely Gaussian (see online material).

The true novelty of the present fit is of course the unambiguous detection of the orbital eccentricity together with the detection of a large orbital precession (see table 1). The value of the measured eccentricity is somewhat larger that what was hinted at in previous works (Shaifullah et al. (2016); Lazaridis et al. (2011); Doroshenko et al. (2001); Stappers et al. (1998)). This is consistent with the idea raised in Voisin et al. (2019) that an unaccounted large precession averages out the eccentricity over the time scale of a precession period (~ 5 years in the present case), in the sense that the envelope of a precessing eccentric orbit is a circle. This idea is reinforced by the finding of Shaifullah et al. (2016) of an apparently variable eccentricity vector when fitting independently small subsets of times of arrival. Further, our assumption that precession is primarily caused by a large gravitational quadrupole moment of the companion star is supported by the negative sign of the precession rate. Indeed, the other source of precession in the model, namely relativistic precession, can only contribute a positive term to the total rate (see also table 1).

The knowledge of the mass ratio q and the inclination of the system $\sin i$ is needed to derive the quadrupole parameters J_s and J_t. In the case of PSR J2051-0827 these parameters were estimated from optical observations of the companion in Stappers et al. (2001), although with important uncertainties (see also below). Fortunately, the facts that quadrupole-induced precession here dominates over relativistic precession ($16J_t \gg 3\epsilon$) and that the mass ratio is very small, $q \ll 1$, render the derivation of the quadrupole parameters little dependent on the values and uncertainties of q and $\sin i$. In other words, to first order one has $J_t \simeq \dot{\omega}/(16 n_b)$. To go further, we use a conservative estimate of the pulsar mass range and of the inclination of the system (Stappers et al. 2001) (see caption of table 1).

In the same manner we determine the minimum eccentricity $e_{\rm min}$, equation (3), and the Keplerian eccentricity e_K. It is interesting to note that the orbit is not perfectly circularised since e_K accounts for nearly half of the total eccentricity. This can be used to derive an eccentricity age (Voisin et al. 2019), $\tau_e = \tau_c \log_{10}(1/e_K)$, where τ_c is the circularisation time-scale (see Hurley et al. (2002) or Voisin et al. (2019)) depending on the component masses and the companion surface temperature. The eccentricity age gives an upper bound on the time needed for the orbit to circularise assuming only tidal forces are at work and an initial eccentricity of 1. For PSR J2051-0827 we calculate the range $\tau_e = 1.6 - 4.1 \cdot 10^8$ years where the uncertainty comes primarily from the masses as well as from the night-side temperature of the companion which we take to be $T_c = 2600 - 3200$K (Stappers et al. 2001). Unless another effect pumps up eccentricity in this system, one should therefore conclude that the system has been in the black-widow state for at most a few hundred million years, and likely much less than that.

Of particular interest is the estimate of the apsidal motion constant k_2 since it can be directly related to the internal structure using stellar models. Unfortunately, our knowledge of the filling factor of the companion star, to which k_2 is extremely sensitive, is very poor since it essentially ranges from 0.2 to 1. Indeed, Stappers et al. (2001) found that due to the asymmetry of the light curve two solutions were possible: one fitting well when only one-half of the light curve was considered (reduced $\chi^2 = 0.96$) yielding a filling factor $f = 0.43^{+0.23}_{-0.16}$, and another fitting the full light curve albeit poorly (reduced $\chi^2 = 5.6$) with a filling factor $f = 0.95^{+0.05}_{-0.02}$. Therefore, we show on figure 1 the value taken by k_2 as a function of the filling factor. We find that a broad range of stellar structures are possible, since $10^{-3} \leq k_2 \leq 0.3$. As a reference, the Sun has an intermediate $k_2 \simeq 0.03$. The record low is held, to our knowledge, by cataclysmic-variable companions (Warner 1978) with $k_2 \sim 10^{-3}$ although these may be more similar to redback companions in terms of mass and evolution. The record high is held by hot Jupiters which have been theoretically shown (Ogilvie 2014; Kramm et al. 2012) to reach $k_2 \sim 0.2$ [4] and are arguably closer to black-widow companions in terms of mass and night-side temperature.

[1] The data processed here is available as an online additional material to Shaifullah et al. (2016) at http://www.epta.eu.org/aom.html.

[2] The timing model implementation is available here : https://bitbucket.org/astro_guillaume_voisin/spider_timing_model/

[3] Our MCMC implementation, with bindings to Tempo2, is available here : https://bitbucket.org/astro_guillaume_voisin/mcmc4tempo2/

[4] There is a factor of 2 compared with the value given in Kramm

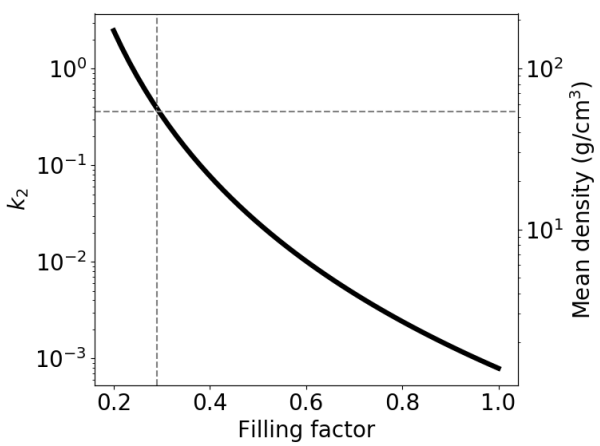

Figure 1. Apsidal motion constant as a function of the filling factor based on the timing results and equation (1). The thickness of the line includes mass ratios from $q = 0.016$ to $q = 0.022$ and is much larger than uncertainties due to parameters derived from timing. The right vertical axis shows the mean density, which curve is identical to that of k_2 with this axis scaling. The horizontal dashed line shows the apsidal motion constant J2051 would have, ~ 0.34, had it the same mean density of 54g/cm^3 as the densest known black-widow companion, PSR J0636+5128 (Kaplan et al. 2018). The vertical dashed line shows the corresponding filling factor which is ~ 0.29.

The latter case would require a small filling factor, typically $f \lesssim 0.5$, compatible with one of the aforementioned light-curve solutions, while a Roche-lobe filling solution, common for spider companions and compatible with the other solution mentioned above, would correspond to a particularly small apsidal motion constant. By comparing the mean density of the companion of PSR J2051-0827 as a function of its filling factor to the mean density of the densest black-widow companion PSR J0636+5128 (Kaplan et al. 2018) we obtain an upper limit $k_2 \sim 0.34$ for a filling factor $f \sim 0.29$ (see figure 1). However, Kaplan et al. (2018) (their figure 4) show a broad scattering of the mean densities from $\sim$ 1g/cm^3 to $\sim$ 54g/cm^3, preventing any more accurate estimate with this criterion.

We show on figure 2 the evolution of the variable quadrupole component according to equation (2) and compare it to the the curve obtained using the BTX fit of Shaifullah et al. (2016). Although broadly consistent, the two versions show significant differences which cannot be straightforwardly explained by the inclusion of new parameters since no correlations are expected between eccentricity, orbital precession and orbital period derivatives (Voisin et al. 2019). This is confirmed by our MCMC fit (see online material). The amplitude of the variations, defined as $\|J_\nu\| = \max(J_\nu) - \min(J_\nu)$, are $\|J_\nu\| \simeq 4.8 \cdot 10^{-8}$ and down to $\|J_\nu\| \simeq 3.4 \cdot 10^{-8}$ if one neglects the edges of the time domain which might be subject to boundary effects. As a consequence, the variable quadrupole component is nearly 100 times smaller than the tidally induced component.

et al. (2012) due to a different definition of the apsidal motion constant. See also Voisin et al. (2019).

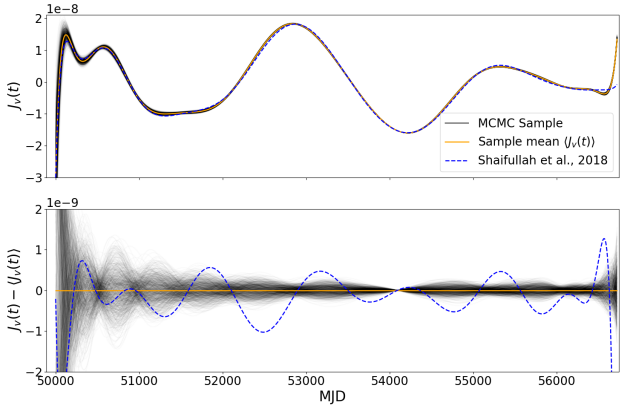

Figure 2. Upper panel : Variable quadrupole parameter $J_\nu(t)$ calculated using equation (2). The mean solution corresponding to table 1 is shown in solid orange, while 1000 lines drawn from the MCMC sample are shown in shades of black. For comparison, the solution of Shaifullah et al. (2016) is shown in dashed blue. Lower panel : difference between the previously mentioned curves and the mean solution, with the same colour code.

4 CONCLUSIONS

We have applied a new timing model accounting for the effects of centrifugally and tidally induced quadrupole deformations of the companion star to the black-widow pulsar PSR J2051-0827, re-analysing the data published in (Shaifullah et al. 2016). This allowed us to make the first unambiguous detection of orbital eccentricity in this system, associated with a large orbital precession due to the quadrupole moment. In addition, the model accounts for orbital period variations by including a time-dependent quadrupole contribution. We could then deduce that this variable component is about 100 times smaller than the combination of tidal and centrifugal deformations. We show that, in principle, these results could be used to derive the apsidal motion constant of the companion star (figure 1) and thus open a new window on the internal structure of these exotic objects. However that will require high-quality optical light curves in order to determine the filling factor of the companion within a few-percent uncertainty, which is not out of reach of current instruments.

ACKNOWLEDGEMENTS

The authors acknowledge support of the European Research Council, under the European Union's Horizon 2020 research and innovation programme (grant agreement No. 715051; Spiders).

REFERENCES

Alpar M. A., Cheng A. F., Ruderman M. A., Shaham J., 1982, Nature, 300, 728
Applegate J. H., 1992, The Astrophysical Journal, 385, 621
Archibald A. M., et al., 2009, Science, 324, 1411
Bassa C. G., et al., 2014, Monthly Notices of the Royal Astronomical Society, 441, 1825

Bassa C. G., et al., 2017, The Astrophysical Journal, 846, L20
Benvenuto O. G., De Vito M. A., Horvath J. E., 2012, The Astrophysical Journal, 753, L33
Breton R. P., et al., 2013, The Astrophysical Journal, 769, 108
Chen H.-L., Chen X., Tauris T. M., Han Z., 2013, The Astrophysical Journal, 775, 27
Damour T., Deruelle N., 1985, Ann. Inst. Henri Poincaré Phys. Théor., Vol. 43, No. 1, p. 107 - 132, 43, 107
Damour T., Deruelle N., 1986, Annales de l'institut Henri Poincaré (A) Physique théorique, 44, 263
Doroshenko O., Löhmer O., Kramer M., Jessner A., Wielebinski R., Lyne A. G., Lange C., 2001, Astronomy and Astrophysics, 379, 579
Edwards R. T., Hobbs G. B., Manchester R. N., 2006, Monthly Notices of the Royal Astronomical Society, 372, 1549
Eggleton P. P., 1983, The Astrophysical Journal, 268, 368
Foreman-Mackey D., Hogg D. W., Lang D., Goodman J., 2013, Publications of the Astronomical Society of the Pacific, 125, 306
Goodman J., Weare J., 2010, Communications in Applied Mathematics and Computational Science, 5, 65
Hessels J. W. T., Ransom S. M., Stairs I. H., Freire P. C. C., Kaspi V. M., Camilo F., 2006, Science, 311, 1901
Hobbs G. B., Edwards R. T., Manchester R. N., 2006, Monthly Notices of the Royal Astronomical Society, 369, 655
Hurley J. R., Tout C. A., Pols O. R., 2002, Monthly Notices of the Royal Astronomical Society, 329, 897
Kaplan D. L., Stovall K., van Kerkwijk M. H., Fremling C., Istrate A. G., 2018, The Astrophysical Journal, 864, 15
Kopal Z., 1978, Dynamics of Close Binary Systems. Springer Netherlands, Dordrecht, http://dx.doi.org/10.1007/978-94-009-9780-6
Kramm U., Nettelmann N., Fortney J. J., Neuhäuser R., Redmer R., 2012, Astronomy and Astrophysics, 538, A146
Lanza A. F., 2006, Monthly Notices of the Royal Astronomical Society, 373, 819
Lanza A. F., Rodonò M., 1999, Astronomy and Astrophysics, 349, 887
Lazaridis K., et al., 2011, Monthly Notices of the Royal Astronomical Society, 414, 3134
Navarrete F. H., Schleicher D. R. G., Käpylä P. J., Schober J., Völschow M., Mennickent R. E., 2019, Monthly Notices of the Royal Astronomical Society
Ogilvie G. I., 2014, Annual Review of Astronomy and Astrophysics, 52, 171
Papitto A., et al., 2013, Nature, 501, 517
Roberts M. S., 2012, Proceedings of the International Astronomical Union, 8, 127
Shaifullah G., et al., 2016, Monthly Notices of the Royal Astronomical Society, 462, 1029
Stappers B. W., Bailes M., Manchester R. N., Sandhu J. S., Toscano M., 1998, The Astrophysical Journal, 499, L183
Stappers B. W., van Kerkwijk M. H., Bell J. F., Kulkarni S. R., 2001, The Astrophysical Journal, 548, L183
Sterne T. E., 1939, Monthly Notices of the Royal Astronomical Society, 99, 451
Voisin G., Breton R. P., Summers C., 2019, Monthly Notices of the Royal Astronomical Society
Völschow M., Schleicher D. R. G., Banerjee R., Schmitt J. H. M. M., 2018, Astronomy and Astrophysics, 620, A42
Warner B., 1978, Acta Astronomica, 28, 303
van Kerkwijk M. H., Breton R. P., Kulkarni S. R., 2011, The Astrophysical Journal, 728, 95

This paper has been typeset from a TEX/LATEX file prepared by the author.

Parameter	Value
MJD range	49989.9-56779.3
NToA	11391
Red. χ^2	4.06
RAJ (rad)	$5.459064089(37)^{+22}_{-21}$
DECJ (rad)	$-0.147663345(83)^{+71}_{-79}$
μ_α (mas/yr)	$5.6(24)^{+14}_{-12}$
μ_δ (mas/yr)	$3.5(29)^{+42}_{-48}$
f (s^{-1})	$2.21796283653060(66)^{+22}_{-17} \cdot 10^{2}$
$\dot{f}$ (s^{-2})	$-6.2649(75)^{+11}_{-12} \cdot 10^{-16}$
f_b (s^{-1})	$1.167797941(44)^{+28}_{-25} \cdot 10^{-4}$
$f_b^{(1)}$ (s^{-2})	$8.(92)^{+18}_{-15} \cdot 10^{-20}$
$f_b^{(2)}$ (s^{-3})	$-7.(836)^{+85}_{-100} \cdot 10^{-27}$
$f_b^{(3)}$ (s^{-4})	$-1.0(84)^{+66}_{-78} \cdot 10^{-34}$
$f_b^{(4)}$ (s^{-5})	$5.(68)^{+35}_{-29} \cdot 10^{-42}$
$f_b^{(5)}$ (s^{-6})	$3.(77)^{+30}_{-25} \cdot 10^{-49}$
$f_b^{(6)}$ (s^{-7})	$(7.1)^{+9.9}_{-12} \cdot 10^{-58}$
$f_b^{(7)}$ (s^{-8})	$-1.(359)^{+91}_{-110} \cdot 10^{-63}$
$f_b^{(8)}$ (s^{-9})	$-2.(79)^{+38}_{-32} \cdot 10^{-71}$
$f_b^{(9)}$ (s^{-10})	$4.(25)^{+34}_{-28} \cdot 10^{-78}$
$f_b^{(10)}$ (s^{-11})	$1.(37)^{+10}_{-12} \cdot 10^{-85}$
$f_b^{(11)}$ (s^{-12})	$-1.0(59)^{+73}_{-88} \cdot 10^{-92}$
$f_b^{(12)}$ (s^{-13})	$-4.(91)^{+36}_{-33} \cdot 10^{-100}$
$f_b^{(13)}$ (s^{-14})	$1.(73)^{+15}_{-12} \cdot 10^{-107}$
$f_b^{(14)}$ (s^{-15})	$1.2(48)^{+91}_{-79} \cdot 10^{-114}$
$f_b^{(15)}$ (s^{-16})	$-5(.8)^{+1.1}_{-1.1} \cdot 10^{-123}$
$f_b^{(16)}$ (s^{-17})	$-1.(69)^{+10}_{-12} \cdot 10^{-129}$
$f_b^{(17)}$ (s^{-18})	$-3.(19)^{+20}_{-23} \cdot 10^{-137}$
x (lt-s)	$4.50705(42)^{+86}_{-89} \cdot 10^{-2}$
$\dot{x}$ (lt-s/s)	$1.0(75)^{+50}_{-55} \cdot 10^{-14}$
$\dot{\omega}$ (deg/yr)	$-68.(56)^{+91}_{-49}$
$T_{\rm asc}$ (MJD)	$5.40910343493(32)^{+68}_{-58} \cdot 10^{4}$
κ_s ($e \sin\omega$)	$-8(.2)^{+1.9}_{-2.4} \cdot 10^{-6}$
κ_c ($e \cos\omega$)	$4.(07)^{+11}_{-13} \cdot 10^{-5}$
Derived quantities	
e	$4.(17)^{+11}_{-11} \cdot 10^{-5}$
$e_{\rm min}$	$2.2(03)^{+14}_{-14} \cdot 10^{-5}$
e_K	$1.(96)^{+11}_{-11} \cdot 10^{-5}$
J_t	$-3.9(08)^{+94}_{-88} \cdot 10^{-6}$
J_s	$-1.3(26)^{+22}_{-21} \cdot 10^{-6}$
ϵ	$3.(52)^{+35}_{-37} \cdot 10^{-6}$
$\dot{\omega}_{\rm rel}$ (deg/yr)	$14.3^{+1.9}_{-2.0}$
$\dot{\omega}_{\rm spin}$ (deg/yr)	$-5.28^{+0.12}_{-0.11}$
$\dot{\omega}_{\rm tid}$ (deg/yr)	$-77.78^{+1.9}_{-1.8}$

Table 1. Results of the MCMC fit of the timing data: mean values of the posterior distribution function are given together with their 68% confidence regions. These error bars apply to the digits between parenthesis and to the full number otherwise. The derived quantities other than the eccentricity e have been sampled assuming a uniform distribution of pulsar masses between $1.3M_\odot$ and $2.4M_\odot$ and a $\cos i$ distribution uniform between 0.4 and 0.8 corresponding to a mean inclination angle $i \simeq 52\,$deg compatible with Stappers et al. (2001). Thus, error bars on derived quantities are conservative.